Differences in the microarchitectural features of the lateral collapsed lesion between osteonecrosis and subchondral insufficiency fracture of the femoral head

河野, 紘一郎

Bone 141 (2020) 115585

Contents lists available at ScienceDirect

Bone

journal homepage: www.elsevier.com/locate/bone

Full Length Article

Differences in the microarchitectural features of the lateral collapsed lesion between osteonecrosis and subchondral insufficiency fracture of the femoral head

Koichiro Kawano, Goro Motomura*, Satoshi Ikemura, Ryosuke Yamaguchi, Shoji Baba, Mingjian Xu, Yasuharu Nakashima

Department of Orthopaedic Surgery, Graduate School of Medical Sciences, Kyushu University, 3-1-1 Maidashi, Higashi-ku, Fukuoka 812-8582, Japan

ARTICLE INFO

Keywords:
Osteonecrosis of the femoral head
Subchondral insufficiency fracture of the femoral head
Microarchitecture
Collapse

ABSTRACT

Background: Like osteonecrosis of the femoral head (ONFH), subchondral insufficiency fracture of the femoral head (SIF) causes femoral head collapse. However, little is known about the differences between the two diseases regarding the morphological features of the collapsed lesion. We tested the hypothesis that the morphological features of the lateral collapsed lesion would differ between ONFH and SIF.

Methods: Twenty femoral heads histopathologically diagnosed as ONFH (n = 10) or SIF (n = 10) were used in this study. In the lateral collapsed lesion of each femoral head, cubic regions of interest (ROIs) were selected within the collapsed subchondral area and the nearby non-collapsed subchondral area. Micro-CT-based microarchitectural parameters were compared between the ROIs in each disease. Additionally, correlations between histopathological and microarchitectural features were evaluated.

Results: In ONFH, bone volume fraction, trabecular thickness, and bone mineral density in the collapsed area were all significantly lower than those in the nearby non-collapsed area where thickened bone trabeculae accompanied by appositional bone formation were invariably seen. On the other hand, in SIF there were no significant differences between the ROIs in any of these microarchitectural parameters. Histopathologically, varying degrees of callus formation overlying the fracture of the subchondral plate were seen around the lateral collapsed lesion.

Conclusion: The morphological features of the lateral collapsed lesion were inconsistent between ONFH and SIF, suggesting different pathomechanisms of femoral head collapse.

1. Introduction

Collapse of the femoral head is a well-known condition that leads to deterioration of the hip joint [1,2] and is most commonly caused by osteonecrosis of the femoral head (ONFH) [3]. Although the precise pathomechanisms of femoral head collapse in ONFH have not been fully elucidated, several studies have demonstrated the significance of the lateral boundary of the necrotic lesion in terms of the risk of collapse. A previous study of femoral head specimens demonstrated that collapse was consistently associated with subchondral fracture at the lateral boundary of the necrotic lesion [4]. In a finite element analysis study, stress was found to be concentrated at the lateral boundary of the femoral head surface before collapse, where sclerotic rim changes were confirmed [5]. These findings suggest that stress concentrated at the lateral boundary causes shear stress between the thickened trabeculae of the reparative zone and the nearby necrotic trabeculae, resulting in subchondral fracture.

Subchondral insufficiency fracture of the femoral head (SIF) has recently come to be recognized as one of the conditions causing femoral head collapse [6,7]. SIF is characterized by acute hip pain without antecedent trauma, and is more common in osteoporotic elderly patients than in younger patients. Although SIF and ONFH share similar radiological findings, such as the crescent sign, the cut section of the femoral head in SIF is quite different from that in ONFH. Specifically,

* Corresponding author at: Department of Orthopaedic Surgery, Graduate School of Medical Sciences, Kyushu University, 3-1-1 Maidashi, Higashi-ku, Fukuoka 812-8582, Japan.

E-mail addresses: kawano7@ortho.med.kyushu-u.ac.jp (K. Kawano), goromoto@ortho.med.kyushu-u.ac.jp (G. Motomura), sikemura@ortho.med.kyushu-u.ac.jp (S. Ikemura), yamaryo@ortho.med.kyushu-u.ac.jp (R. Yamaguchi), s-baba@ortho.med.kyushu-u.ac.jp (S. Baba), yasunaka@ortho.med.kyushu-u.ac.jp (Y. Nakashima).

https://doi.org/10.1016/j.bone.2020.115585
Received 22 May 2020; Received in revised form 3 August 2020; Accepted 9 August 2020
Available online 12 August 2020

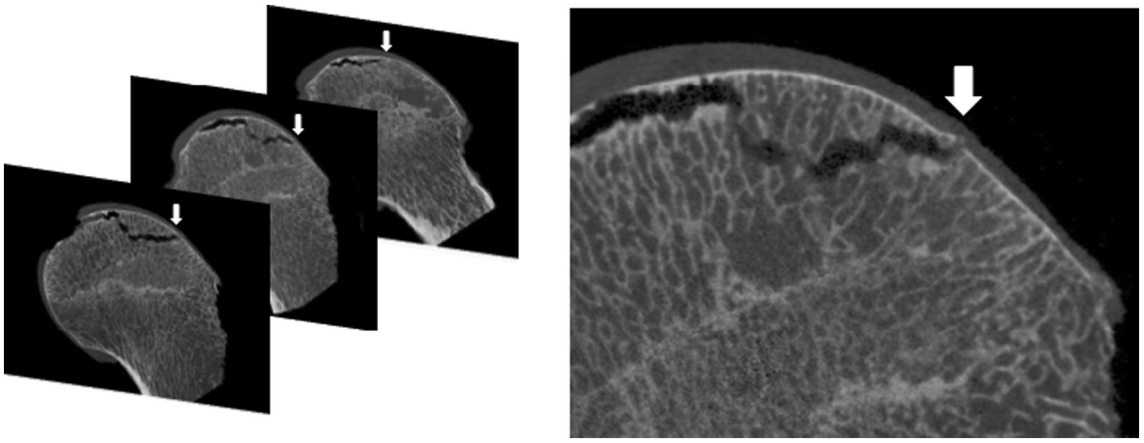

Fig. 1. Using micro-CT, the lateral collapsed lesion was defined as the lateral subchondral region that included a fracture of the subchondral plate (white arrow).

while wedged-shaped opaque yellow region is typically observed in ONFH [1], it is never seen in SIF [8]. Histologically, SIF is characterized by fracture callus accompanied by granulation tissue around the subchondral fractured area [8]. Although small foci of necrosis are often observed in the collapsed lesion, the absence of a primary osteonecrotic lesion surrounded by a reparative zone is a feature of SIF that distinguishes it from ONFH [9].

Recently, the examination of bone microarchitecture by micro-computed tomography (CT) has been used to evaluate the morphological features of cancellous bones [10,11]. Since this microarchitecture is considered to be correlated with bone strength [12], assessing it in the location of the collapsed lesion may clarify how specific diseases result in femoral head collapse.

No studies thus far have focused on differences in the microarchitectural features of the collapsed lesion between ONFH and SIF. Since the lateral collapsed lesion is considered to be a key region in SIF [13,14], we hypothesized that morphological features at the lateral collapsed lesion might differ between ONFH and SIF. In this study, we compared the characteristics of the bone microarchitecture at the lateral collapsed lesion in both diseases.

2. Materials and methods

2.1. Materials

Our institutional review board approved this study, and written informed consent was obtained from all patients in accordance with the Declaration of Helsinki. The inclusion criteria for the femoral heads in this study were: (1) histopathological diagnosis as ONFH or SIF, and (2) less than 3-mm depth of collapse. We reviewed 150 consecutive patients with ONFH and 35 consecutive patients with SIF who underwent total hip arthroplasty between October 2010 and September 2019. A total of 117 hips with ONFH and 25 hips with SIF were excluded from the study due to the presence of osteoarthritic changes or severe femoral head collapse (depth greater than 3 mm). Of the remaining 33 hips with ONFH, 23 were excluded due to unavailable specimens or micro-CT data. Finally, 20 femoral heads that were histopathologically diagnosed as ONFH (n = 10) or SIF (n = 10) were used in this study. ONFH was defined by a zonal pattern comprising an area of bone infarction, reparative granulation, and viable tissue [15]. SIF was defined by a whitish-gray area consisting of irregularly arranged fracture callus, reactive cartilage, and granulation tissue [6,8,9]. Although small areas of necrotic bone trabeculae and bone marrow may be observed in SIF, such necrosis is confined to the area around the fracture line that shows no evidence of antecedent bone infarction [1,8,9]. Histopathological diagnosis was achieved by consensus by two observers with extensive relevant experience. ONFH patients consisted of eight males and two females with a mean age of 44 years (range: 34–55 years). SIF patients consisted of two males and eight females with a mean age of 70 years (range: 52–84 years). Five resected femoral heads from patients with femoral neck fracture (FNF) were used as a control; these patients consisted of four males and one female with a mean age of 69 years (range: 59–75 years). In ONFH, four patients had a history of corticosteroid pulse therapy, and one of these patients was still receiving corticosteroids at the time of surgery. Both a bisphosphonate and vitamin D were administered to two patients with a history of corticosteroid treatment. In SIF, a selective estrogen receptor modulator was administered to one patient, and vitamin D was administered to two patients. In the control, none of the patients were receiving medication that may have affected bone metabolism. The mean duration from pain onset to surgery was 6.4 months (range: 2–14 months) in ONFH, and 2.9 months (range: 2–5 months) in SIF. In addition, the location of the necrotic lesion in ONFH was classified using the Japanese Investigation Committee classification system [16], as follows: type C1 in four hips and type C2 in six hips.

2.2. Lateral collapsed lesion on micro-CT

All femoral heads were scanned with high-resolution micro-CT (R_mCT T1; Rigaku, Tokyo, Japan) immediately after harvest. Scanning was performed with a voltage of 60 kV, current of 60 μA, resolution of 50 μm per pixel, and slice thickness of 0.4 mm.

A lateral collapsed lesion was defined as a subchondral region that included a fracture of the subchondral plate, and that was clearly identified on sequential coronal micro-CT slices (Fig. 1). First, we evaluated whether a lateral collapsed lesion was present anywhere on the femoral head. Since the lateral collapsed lesion was commonly observed at the central coronal slice area in all 20 femoral heads, the microarchitecture and histopathology of this area were evaluated. Additionally, we evaluated the condition of the medial portion of the collapsed lesion.

2.3. Microarchitectural examination

We set two pairs of 5-mm cubic regions of interest (ROIs) around the lateral collapsed lesion in the central portion. Two ROIs were set adjacent to the fracture of the subchondral plate, one in the collapsed area and the other in the non-collapsed area (Fig. 2). In control femoral heads, two adjacent cubic ROIs were set at the lateral area corresponding to the site of the lateral collapsed lesion in non-control femoral heads (Fig. 2).

The bone microarchitecture of the lateral collapsed lesion was assessed using a 3D image analysis system (TRI/3D-BON; RATOC System Engineering, Tokyo, Japan) using a reference phantom (Kyoto Kagaku,

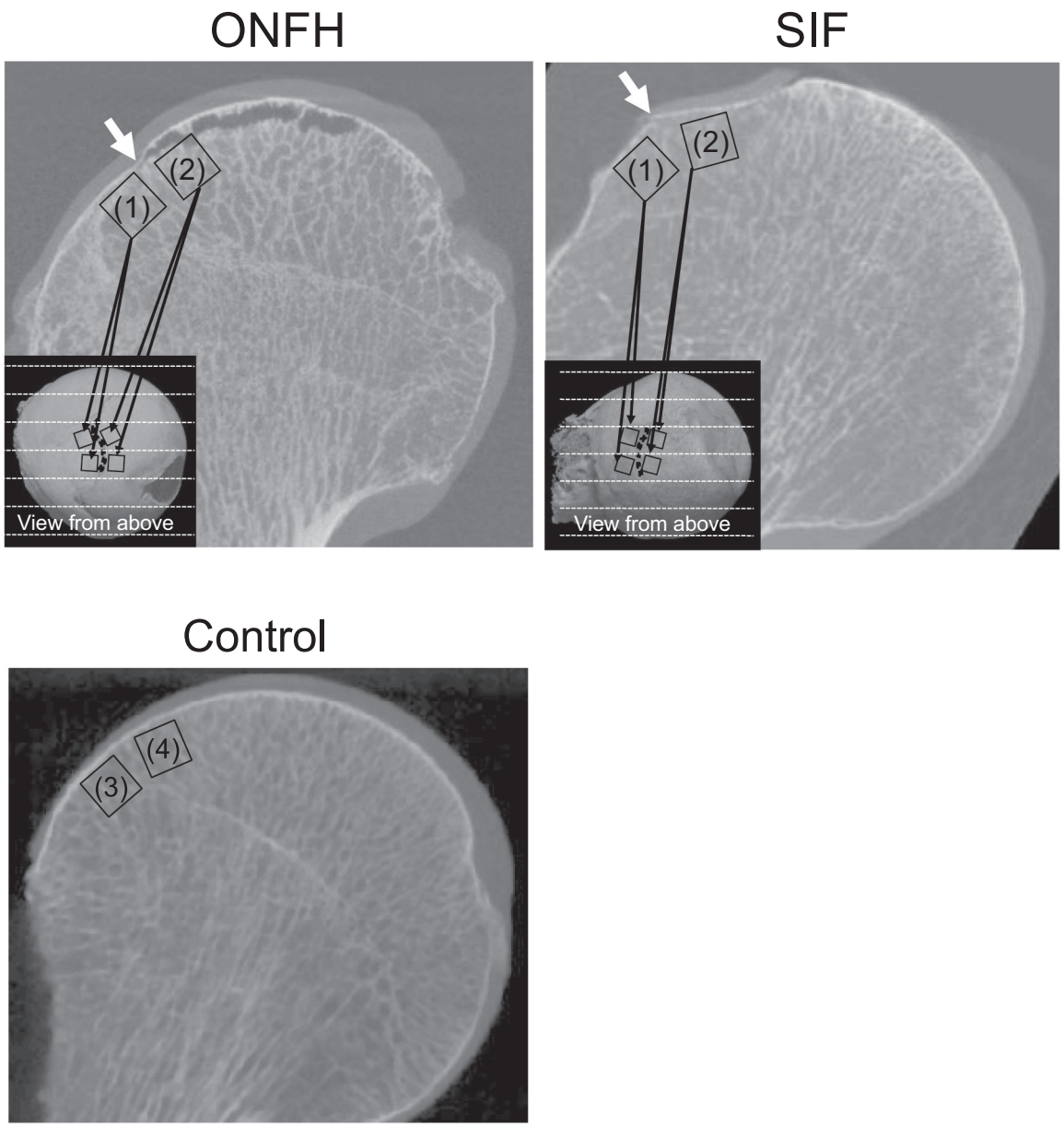

Fig. 2. Two-dimensional micro-CT images show central slices of the femoral head in osteonecrosis of the femoral head (ONFH) and subchondral insufficiency fracture of the femoral head (SIF). White arrows indicate a fracture of the subchondral plate. For microarchitectural analysis, regions of interest consisting of two 5-mm cubes were defined in each of two subchondral areas of the femoral head: (1) the non-collapsed area and (2) the nearby collapsed area. In the controls, two pairs of adjacent cubic ROIs were defined in the lateral area, corresponding to (3) the non-collapsed area and (4) the collapsed area in SIF. The black dotted line in the 3-dimensional micro-CT image indicates a fracture line of the subchondral plate.

Kyoto, Japan) [17]. In each of the diseases, the following bone parameters were compared between the ROIs of adjacent subchondral areas: bone volume fraction (BV/TV), trabecular thickness (Tb.Th), trabecular separation (Tb.Sp), and bone mineral density (BMD) [18].

2.4. Histopathological examination

After micro-CT scanning, all femoral heads were fixed in 4% paraformaldehyde for three days and soaked in 70% ethanol for one day to remove fat from the bone marrow, then cut along the coronal plane into 3-mm-thick sections parallel to the cervical axis. Thereafter, the samples were decalcified using EDTA for seven days, embedded in paraffin, and cut into 3-μm-thick sections. Hematoxylin and eosin (HE) staining was performed to evaluate the histopathological appearance in the mid-coronal slices of the femoral heads. Evaluation areas of 5 mm square were selected in both the collapsed area and the nearby non-collapsed area at the lateral collapsed lesion where the microarchitecture was evaluated on micro-CT. The trabecular thickness, proportion of empty lacunae, and cartilage thickness were evaluated in five randomly selected fields of view. The number of multinuclear giant cells per mm^2 was calculated based on the size of the evaluation area.

2.5. Clinical image evaluation by Hounsfield unit values on CT

To evaluate the BMD of the lateral collapsed lesion, we examined Hounsfield unit (HU) values of plain CT images obtained within a month before surgery [19,20]. We used non-contrast CT images (Aquilion scanner; Toshiba, Tochigi, Japan) using a tube voltage of 120 kVp and 2-mm intervals, with a slice thickness of 0.63 mm. CT images were available for eight patients with ONFH and eight patients

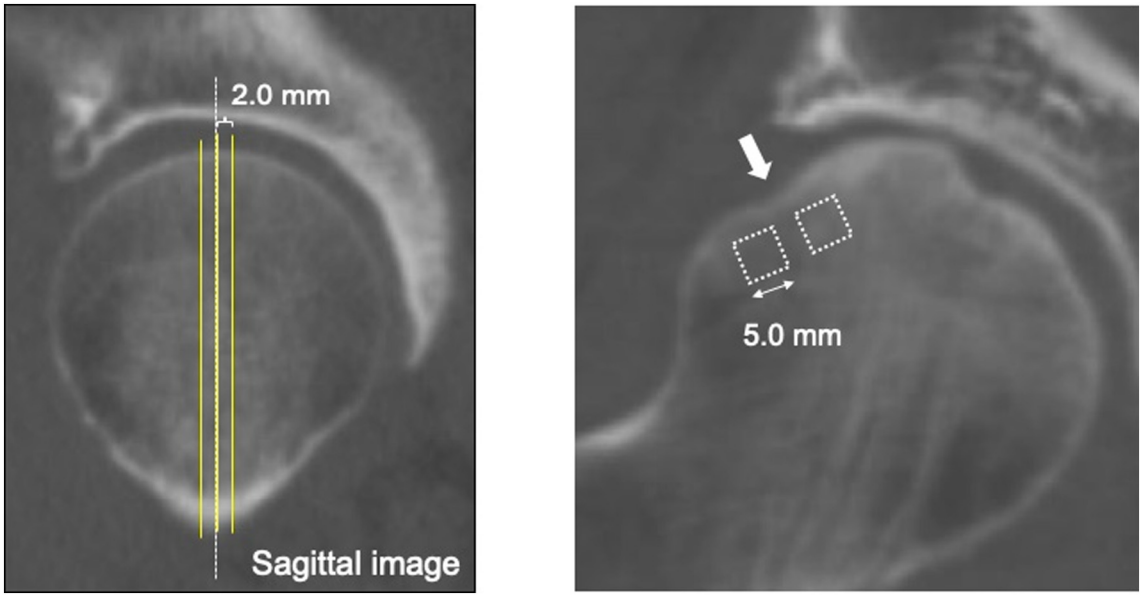

Fig. 3. Defining the region of interest (ROI) for the measurement of Hounsfield unit (HU) values. The ROI was set as two 5.0 mm × 5.0 mm squares, one in the collapsed subchondral area and one in the nearby non-collapsed subchondral area on the central three slices. The white arrow indicates slight depression of the femoral head surface.

with SIF. A 5.0 mm × 5.0 mm square ROI was defined in the collapsed subchondral area and in the nearby non-collapsed subchondral area in each of three sequential coronal slices (Fig. 3). The ROI locations corresponded to the regions used in the aforementioned microarchitectural examination. The HU values of the ROIs were measured using a DICOM viewer (ONIS 2.5 free edition; Digitalcore, Tokyo, Japan). To decrease slice-specific differences, the average HU value of the three slices was used for the examination [20].

2.6. Statistical analysis

Data are expressed as means ± SD. Two observers (KK and MX) independently and blindly evaluated the histopathological parameters at monthly intervals. The intra- and inter-observer reliabilities were assessed using intraclass correlation coefficients. The intraclass correlation was defined as substantial when the value was 0.61–0.80, and as almost perfect when the value was > 0.80.

In each disease, the microarchitectural parameters, histopathological parameters, and HU values were compared between the non-collapsed area and the nearby collapsed area using the Wilcoxon signed-rank test. The Spearman rank correlation coefficient was used to evaluate the correlations between HU values and microarchitectural parameters. The statistical analysis was performed using the JMP 13.0 software package (SAS Institute, Cary, NC, USA). A p-value of < 0.05 was considered to be statistically significant.

3. Results

3.1. Distribution of lateral collapsed lesions

In ONFH femoral heads, the lateral collapsed lesions were widely distributed from the anterior to central portion, whereas they were distributed mainly in the central portion in SIF femoral heads (Fig. 4).

The lateral collapsed lesion had more severe depression than the medial collapsed lesion in all ONFH femoral heads, whereas the medial collapsed lesion had more severe depression in two SIF femoral heads.

3.2. Bone microarchitecture at the lateral collapsed lesion

In ONFH, the values of BV/TV, Tb.Th, and BMD in the non-collapsed area (60.2 ± 9.0%, 612 ± 119 μm, 320 ± 33 mg/cm^3, respectively) were significantly higher than those in the collapsed area (51.7 ± 10.6%, 455 ± 84 μm, and 285 ± 32 mg/cm^3, respectively) ($p < 0.01$, $p < 0.001$, and $p < 0.001$, respectively). There was no significant difference in Tb.Sp between the non-collapsed area (403 ± 150 μm) and the collapsed area (442 ± 149 μm) ($p = 0.32$). On the other hand, in SIF, the values of BV/TV, Tb.Th, Tb.Sp, and BMD showed no significant differences between the non-collapsed area (47.9 ± 13.5%, 486 ± 150 μm, 547 ± 166 μm, and 260 ± 42 mg/cm^3, respectively) and the collapsed area (53.0 ± 10.6%, 492 ± 97 μm, 442 ± 149 μm, and 277 ± 43 mg/cm^3, respectively) ($p = 0.23$, $p = 0.44$, $p = 0.053$, and $p = 0.19$, respectively). In the controls, there was no significant difference in microarchitectural parameters between the two lateral areas, which showed similar trends to SIF (BV/TV: 39.9 ± 13.2% vs 34.0 ± 7.4%, respectively, $p = 0.07$; Tb.Th: 310 ± 74 μm vs 289 ± 45 μm, respectively, $p = 0.11$; Tb.Sp: 520 ± 178 μm vs 575 ± 121 μm, respectively, $p = 0.14$; BMD: 239 ± 37 mg/cm^3 vs 233 ± 31 mg/cm^3, respectively, $p = 0.10$) (Fig. 5).

3.3. Histopathological findings at the lateral collapsed lesion

In ONFH, thickened trabeculae with appositional bone formation were observed in the non-collapsed area (Fig. 6A, B), which was consistent with a significant increase in the trabecular thickness in the non-collapsed area ($p < 0.01$). Massive empty lacunae were observed in the collapsed area, which was consistent with a significant increase in the proportion of empty lacunae in the collapsed area ($p < 0.01$) (Fig. 6A, C). The number of multinuclear giant cells in the non-collapsed area was significantly higher than that in the collapsed area ($p < 0.05$) (Table 1).

In SIF, varying degrees of callus formation and granulation tissue were seen in both the collapsed area and the nearby non-collapsed area around the lateral collapsed lesion (Fig. 6D, E). Regarding histopathological parameters, there were no significant differences between the non-collapsed and nearby collapsed areas in terms of trabecular thickness ($p = 0.19$), proportion of empty lacunae ($p = 0.06$), or cartilage thickness ($p = 0.18$). The number of multinuclear giant cells in the non-collapsed area was significantly lower than that in the collapsed area ($p < 0.01$) (Table 1) (Fig. 6F).

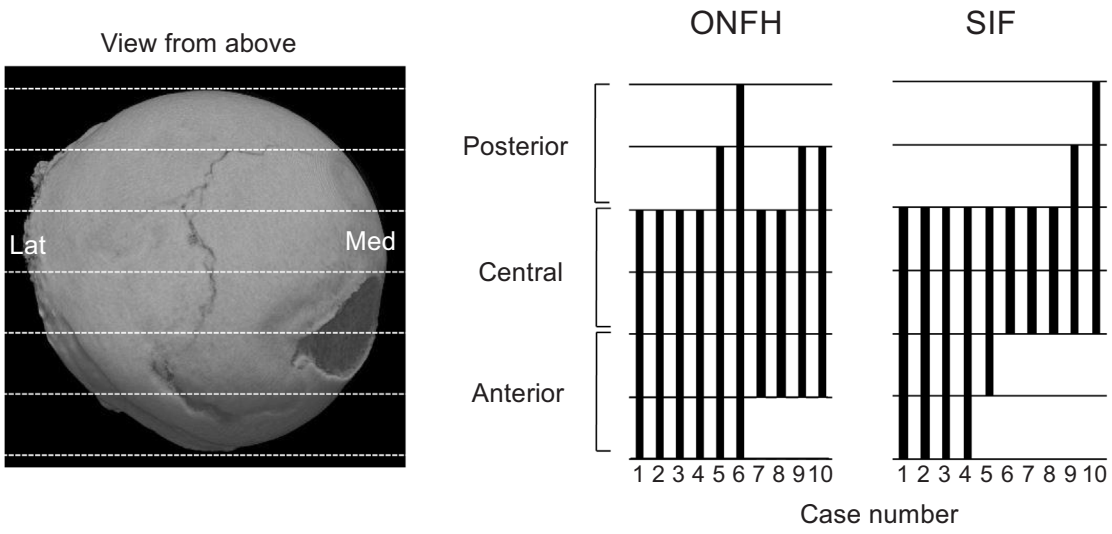

Fig. 4. The distribution of fractures of the subchondral plate in osteonecrosis of the femoral head (ONFH) and subchondral insufficiency fracture (SIF). Bands indicate the anteroposterior distribution of the fracture.

Both the intra- and inter-observer reliabilities of the proportion of empty lacunae, number of multinuclear giant cells, and cartilage thickness were almost perfect (0.85–0.97 and 0.94–0.98, respectively for intra- and inter-observer reliabilities). The intra- and inter-observer reliabilities of the trabecular thickness were substantial (0.68, 0.77, respectively).

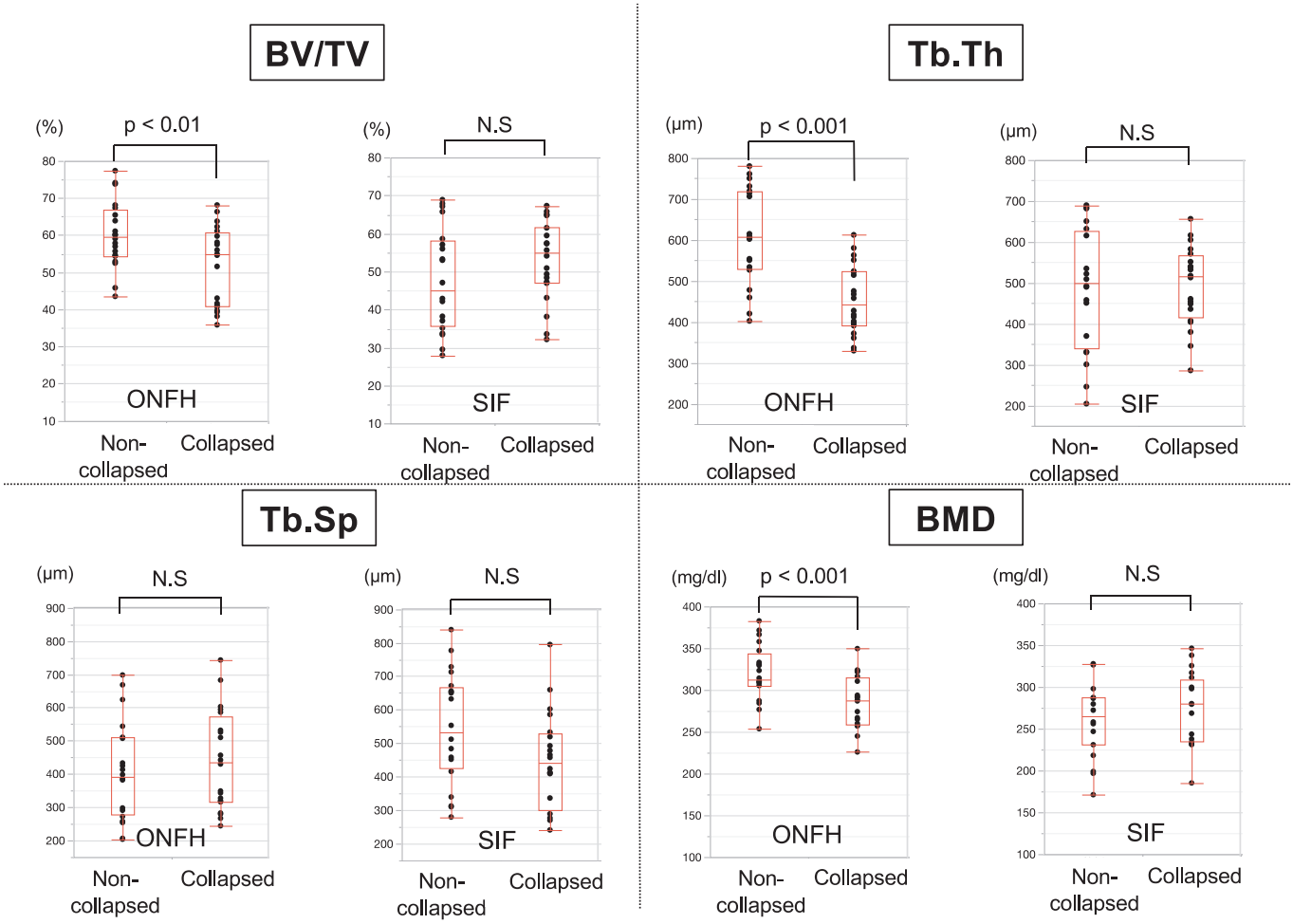

Fig. 5. Comparison of microarchitectural bone parameters between the non-collapsed and collapsed areas in osteonecrosis of the femoral head (ONFH) and subchondral insufficiency fracture of the femoral head (SIF). Statistical significance is defined as $p < 0.05$. BV/TV = bone volume fraction, Tb.Th = trabecular thickness, Tb.Sp = trabecular separation, BMD = bone mineral density.

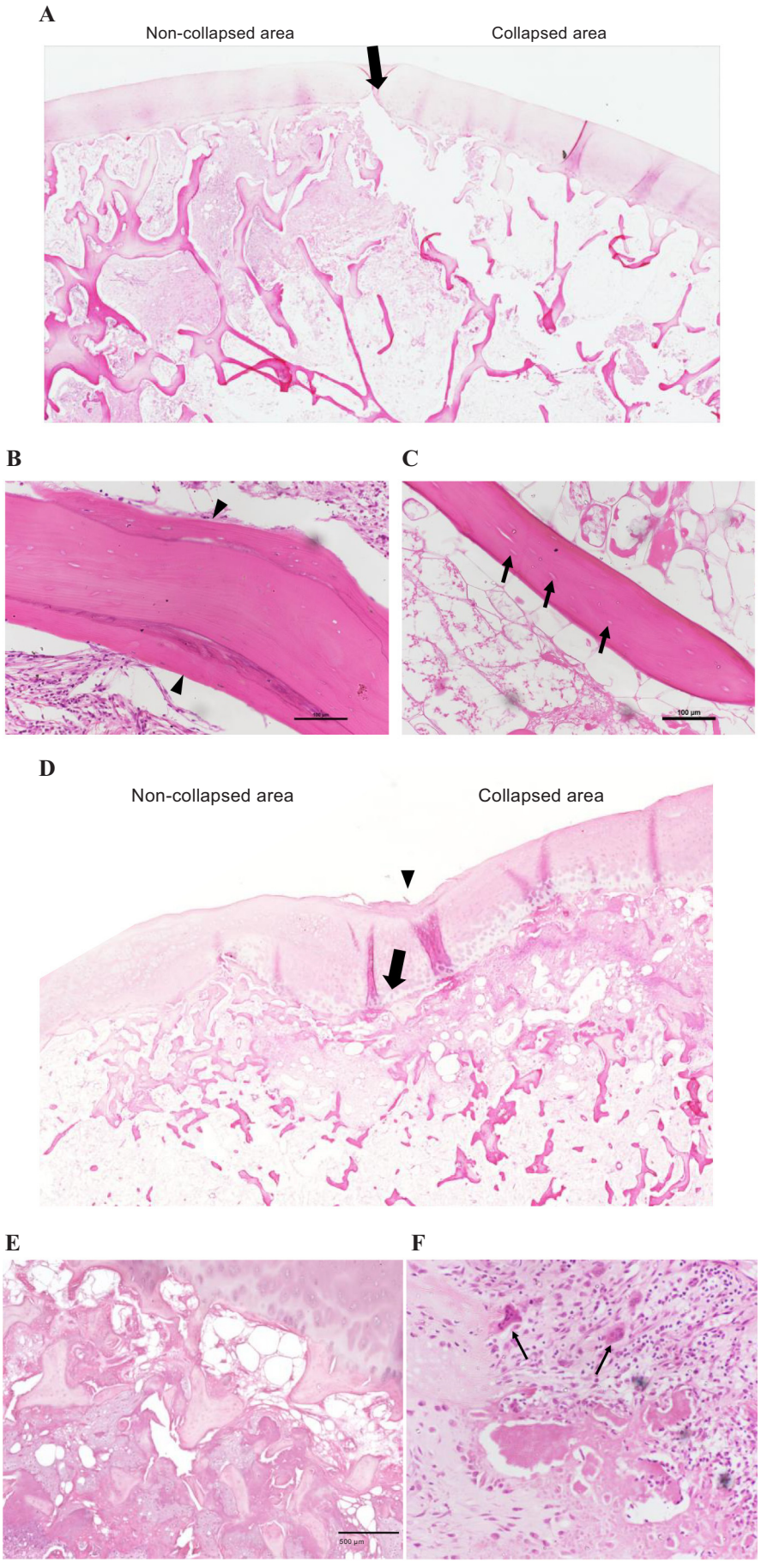

Fig. 6. A Histopathological findings show different findings between the non-collapsed and collapsed areas in osteonecrosis of the femoral head (ONFH). A black arrow indicates the lateral subchondral fracture.
B A thickened trabecula with appositional bone formation (black arrowheads), which is characteristic of the reparative zone in ONFH, is observed in the non-collapsed area.
C The thin trabecula and its massive empty lacunae (black arrows), which are characteristic of the necrotic zone in ONFH, is observed in the collapsed area.
D The histopathological findings are similar between the non-collapsed and collapsed areas in subchondral insufficiency fracture of the femoral head (SIF). Callus formation like bridging callus overlying a fracture of the subchondral plate is observed around the lateral collapsed lesion. A black arrowhead indicates the depression of articular cartilage associated with the lateral collapsed lesion. A black arrow indicates the lateral subchondral fracture.
E Vigorous callus formation is observed in the subchondral area around the lateral collapsed lesion in SIF.
F Numerous multinuclear giant cells are observed in the collapsed area in SIF (black arrows).

Table 1
Comparison of histopathological findings between the non-collapsed and collapsed areas in osteonecrosis of the femoral head (ONFH) and subchondral insufficiency fracture of the femoral head (SIF).

	Comparisons between the non-collapsed and collapsed areas					
	ONFH			SIF		
	Non-collapsed area	Collapsed area	*p*	Non-collapsed area	Collapsed area	*p*
Trabecular thickness (μm)	275 ± 77	189 ± 47	< 0.01	218 ± 117	209 ± 100	0.19
Empty lacunae (%)	45 ± 25	82 ± 14	< 0.01	4.2 ± 3.0	6.1 ± 4.4	0.06
Multinuclear giant cell (/mm^2 × 10)	1.1 ± 0.9	0.1 ± 0.4	< 0.05	3.9 ± 2.7	9.7 ± 8.0	< 0.01
Cartilage thickness (μm)	1203 ± 465	1400 ± 456	0.21	1165 ± 403	1355 ± 551	0.18

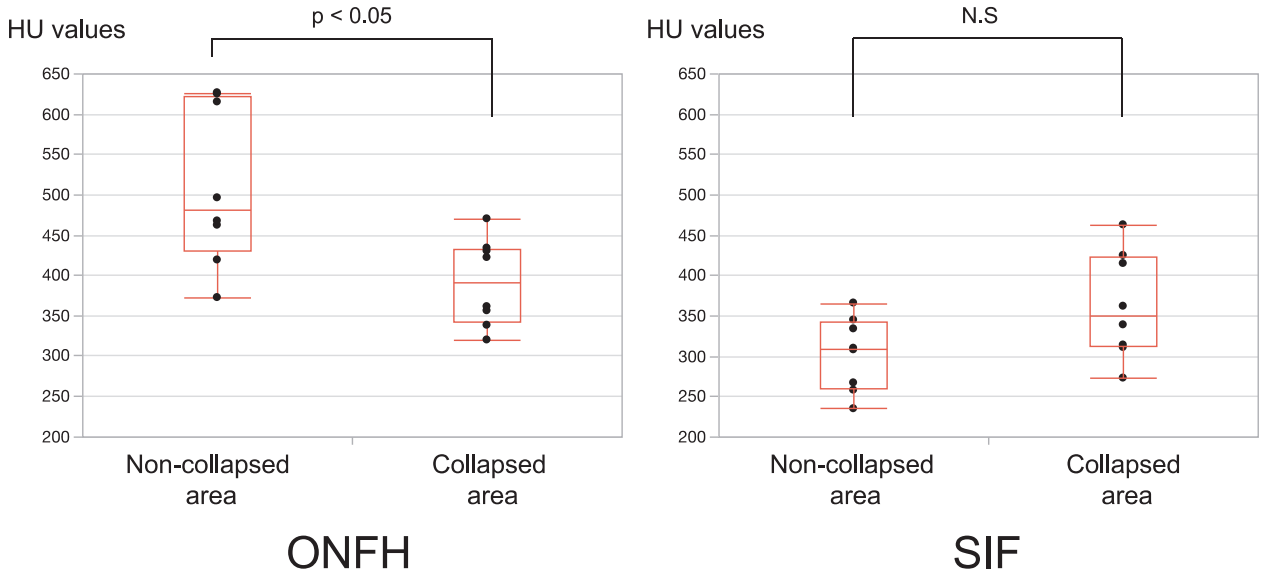

Fig. 7. Comparison of the mean Hounsfield unit (HU) values between the non-collapsed and collapsed areas in osteonecrosis of the femoral head (ONFH) and subchondral insufficiency fracture of the femoral head (SIF). Statistical significance is defined as $p < 0.05$.

3.4. HU values of the lateral collapsed lesion (Fig. 7)

In ONFH, the mean HU value of the non-collapsed area (510 ± 99) was significantly higher than that of the collapsed area (391 ± 54) ($p < 0.05$). On the other hand, in SIF, there was no significant difference between the non-collapsed area (303 ± 46) and the collapsed area (363 ± 66) ($p = 0.07$). The mean HU value of the lateral collapsed lesion showed a significant correlation with the BMD obtained from microarchitectural examination ($r = 0.57$, $p < 0.001$).

4. Discussion

This study is the first to demonstrate morphological differences in the collapsed femoral head between ONFH and SIF by focusing on the lateral collapsed lesion. In ONFH femoral heads, the non-collapsed area and the nearby collapsed area showed significant differences in three microarchitectural parameters, namely BV/TV, Tb.Th, and BMD. These results were supported by histopathological findings of thickened trabeculae accompanied by appositional bone formation in the non-collapsed area, and necrotic bone trabeculae in the collapsed area. Meanwhile, unlike in ONFH, in SIF there were no significant differences in any microarchitectural parameters between the two sides of the lateral collapsed lesion, suggesting that the pathomechanism of collapse in SIF may not be the same as that in ONFH. This difference is suspected to be due to the presence or absence of reparative sclerotic tissues.

Since the current study demonstrated the morphological features of collapsed femoral heads, the differences between diseases may reflect a disparity in the reparative reaction to subchondral fracture. However, in ONFH, the reparative response to osteonecrotic lesions is considered to start before collapse [21]. A previous FEM study also demonstrated a similar stress distribution on the femoral head surface between pre-collapse ONFH with sclerotic boundaries and post-collapse ONFH [5], suggesting the presence of similar morphological features just before and after collapse in ONFH. Although nothing could be elucidated before occurrence of collapse in SIF, we believe that the discrepancies between ONFH and SIF seen in the current study suggest different pathomechanisms of collapse between the diseases.

Considering that SIF can even occur in young patients and is associated with risk factors other than those involving the femoral head, such as hip dysplasia, mechanical stress, and inversion of the acetabular labrum [14,22], it is speculated that a strong focal force causes femoral head collapse in SIF. Surprisingly, there have been few reports on the mechanism of osteoporotic fractures [23], and this remains an unresolved issue. In this study, a histopathological feature of the lateral collapsed lesion in SIF was a larger number of osteoclast-like multinuclear giant cells than in ONFH. Since femoral head collapse generally results in the destruction of numerous bone trabeculae, which induce the recruitment and differentiation of osteoclasts if the area is still viable [24], the increase in the number of multinuclear giant cells in the collapsed area may be a reaction to fractures. Although the mechanism of collapse could not be elucidated from this study, given that bisphosphonates prevent vertebral body fractures by inhibiting bone resorption, trabeculae that are mechanically weakened by osteoclastic bone resorption may cause femoral head collapse in SIF [25]. Further studies using mechanical tests should be performed to elucidate the mechanism of collapse in SIF.

Compared to SIF, the number of multinuclear giant cells in the non-collapsed area was found to be increased in ONFH, which is consistent with a previous report showing that the number of osteoclasts in the reparative zone was significantly higher than that in the necrotic zone [26]. Another study demonstrated that while the osteoclast number was not increased at the non-collapsed sclerotic boundary of the necrotic lesion, it was higher at the collapsed boundary [27]. Considering that the femoral heads evaluated in the current study were already collapsed, we suppose that the increase of multinuclear giant cells in the non-collapsed area in ONFH may be the result of collapse.

HU values on plain CT represent a normalized index of X-ray attenuation based on a scale ranging from −1000 for air to 0 for water [28]. HU values have been shown to correlate with BMD values obtained using various measurement methods, such as dual-energy X-ray absorptiometry and quantitative CT, suggesting their clinical utility [29,30]. In our study, microarchitectural analysis using micro-CT showed that the HU values around the lateral collapsed lesion correlated with BMD. Also, the evaluation using HU values was able to detect the difference between the two sides of the lateral collapsed lesion in ONFH, as seen in the microarchitectural evaluation. In addition, the HU values identified the difference in characteristics of the lateral collapsed lesion between ONFH and SIF, suggesting that plain CT may be a useful tool for distinguishing the two diseases.

Our study has several limitations. First, we analyzed only 10 femoral heads each in SIF and ONFH. The precise histopathological diagnosis of SIF is difficult for femoral heads with severe collapse. To minimize the effect of collapse on the microarchitecture, we focused on cases in which the depth of collapse was less than 3 mm. However, in both diseases it was difficult to obtain femoral heads with only a slight collapse, since in addition to the rarity of SIF, joint-preserving surgery is often performed for ONFH patients with minimal collapse. Despite the small number of cases, it is meaningful to evaluate femoral heads with minimal collapse in accurately diagnosed ONFH or SIF. Second, the patient age distribution differed between SIF and ONFH, which may have affected the microarchitectural results. However, we avoided this problem by evaluating the microarchitectural features of each disease separately rather than in comparison with each other. Third, we evaluated femoral heads that had already collapsed. It is important to evaluate the pathophysiology before collapse to determine the mechanism involved, but it is impossible to identify SIF before collapse. Nonetheless, by focusing on cases with minimal collapse, we succeeded in identifying differences between the two diseases, thus elucidating how features of collapse are impacted by the presence of necrotic lesion surrounded by reparative tissues. Further studies are needed to clarify the mechanism of collapse. Fourth, ONFH and SIF differed regarding medication history and the duration from pain onset to surgery. Although these factors might cause variability in the microarchitectural parameters even in the same disease, we feel that our results are meaningful and provide certain characteristics of microarchitecture in each disease.

In conclusion, the morphological features of the lateral collapsed lesion were inconsistent between ONFH and SIF, suggesting different pathomechanisms of femoral head collapse.

CRediT authorship contribution statement

Koichiro Kawano: Methodology, Investigation, Writing - original draft, Validation. **Goro Motomura:** Methodology, Investigation, Validation. **Satoshi Ikemura:** Investigation, Validation. **Ryosuke Yamaguchi:** Investigation, Validation. **Shoji Baba:** Investigation, Validation. **Mingjian Xu:** Investigation, Validation. **Yasuharu Nakashima:** Investigation, Validation.

Declaration of competing interest

The authors declare that they have no conflicts of interest.

Acknowledgments

This work was supported in part by a research grant from the Japan Society for the Promotion of Science, Japan (JP19K09601).

References

[1] P.G. Bullough, E.F. DiCarlo, Subchondral avascular necrosis: a common cause of arthritis, Ann. Rherum. Dis. 49 (1990) 412–420.
[2] M.A. Mont, L.C. Jones, D.S. Hungerford, Nontraumatic osteonecrosis of the femoral head: ten years later, J. Bone Joint Surg. Am. 85 (2006) 1117–1132.
[3] K. Ohzono, M. Saito, K. Takaoka, K. Ono, S. Saito, T. Nishina, T. Kadowaki, Natural history of nontraumatic avascular necrosis of the femoral head, J. Bone Joint Surg. Br. 73 (1991) 68–72.
[4] G. Motomura, T. Yamamoto, R. Yamaguchi, S. Ikemura, Y. Nakashima, T. Mawatari, Y. Iwamoto, Morphological analysis of collapsed regions in osteonecrosis of the femoral head, J. Bone Joint Surg. Br. 93 (2011) 184–187.
[5] T. Utsunomiya, G. Motomura, S. Ikemura, Y. Kubo, K. Sonoda, H. Hatanaka, S. Baba, K. Kawano, T. Yamamoto, Y. Nakashima, Effects of sclerotic changes on stress concentration in early-stage osteonecrosis: a patient-specific, 3D finite element analysis, J. Orthop. Res. 36 (2018) 3169–3177.
[6] T. Yamamoto, P.G. Bullough, Subchondral insufficiency fracture of the femoral head: a differential diagnosis in acute onset of coxarthrosis in the elderly, Arthritis Rheum. 42 (1999) 2719–2723.
[7] M. Rafii, H. Mitnick, J. Klug, H. Firooznia, Insufficiency fracture of the femoral head: MR imaging in three patients, AJR Am. J. Roentgenol. 168 (1997) 159–163.
[8] T. Yamamoto, Subchondral insufficiency fractures of the femoral head, Clin. Orthop. Surg. 4 (2012) 173–180.
[9] T. Yamamoto, Y. Iwamoto, R. Schneider, P.G. Bullough, Histopathological prevalence of subchondral insufficiency fracture of the femoral head, Ann. Rheum. Dis. 67 (2008) 150–153.
[10] Z.M. Zhang, Z.C. Li, L.S. Jiang, S.D. Jiang, L.Y. Dai, Micro-CT and mechanical evaluation of subchondral trabecular bone structure between postmenopausal women with osteoarthritis and osteoporosis, Osteoporos. Int. 21 (2010) 1383–1390.
[11] R. Hambli, Micro-CT finite element model and experimental varidation of trabecular bone damage and fracture, Bone. 56 (2013) 363–374.
[12] C.H. Turner, Biomechanics of bone: determinants of skeletal fragility and bone quality, Osteoporos. Int. 13 (2002) 97–104.
[13] K. Ishihara, K. Miyanishi, H. Ihara, S. Jingushi, T. Torisu, Subchondral insufficiency fracture of the femoral head may be associated with hip dysplasia: a pilot study, Clin. Orthop. 468 (2010) 1331–1335.
[14] K. Iwasaki, T. Yamamoto, G. Motomura, K. Karasuyama, K. Sonoda, Y. Kubo, Y. Iwamoto, Common site of subchondral insufficiency fractures of the femoral head based on three-dimensional magnetic resonance imaging, Skelet. Radiol. 45 (2016) 105–113.
[15] T. Yamamoto, E.F. DiCarlo, P.G. Bullough, The prevalence and clinic pathological appearance of extension of osteonecrosis in the femoral head, J. Bone Joint Surg. Br. 81 (1999) 328–332.
[16] N. Sugano, T. Atsumi, K. Ohzono, T. Kubo, K. Hotokebuchi, K. Takaoka, The 2001 revised criteria for diagnosis, classification, and staging of idiopathic osteonecrosis of the femoral head, J. Orthop. Sci. 7 (2002) 601–605.
[17] K. Inoue, T. Hamano, N. Nango, I. Matsui, K. Tomida, S. Mikami, N. Fujii, C. Nakano, Y. Obi, A. Shimomura, Y. Kusunoki, H. Rakugi, Y. Isaka, Y. Tsubakihara, Multidetector-row computed tomography is useful to evaluate the therapeutic effects of bisphosphonates in glucocorticoid-induced osteoporosis, J. Bone Miner. Metab. 32 (2014) 271–280.
[18] J.X. Ma, W.W. He, J. Zhao, M.J. Kuang, H.H. Bai, L. Sun, B. Lu, A.X. Tian, Y. Wang, B.C. Dong, Y. Wang, X.L. Ma, Bone microarchitecture and biomechanics of the necrotic femoral head, Sci. Rep. 7 (2017) 13345.
[19] S.Y. Lee, S.S. Kwon, H.S. Kim, J.H. Yoo, J. Kim, J.Y. Kim, B.C. Min, S.J. Moon, K.H. Sung, Reliability and validity of lower extremity computed tomography as a screening tool for osteoporosis, Osteoporos. Int. 26 (2015) 1387–1394.
[20] S. Baba, G. Motomura, S. Ikemura, R. Yamaguchi, T. Utsunomiya, H. Hatanaka, K. Kawano, M. Xu, Y. Nakashima, Is bone mineral density lower in the necrotic lesion in pre-collapse osteonecrosis of the femoral head? J. Orthop. Res. (2020), https://doi.org/10.1002/jor.24674 (Epub ahead of print).
[21] G. Motomura, T. Yamamoto, K. Abe, Y. Nakashima, M. Ohishi, S. Hamai, T. Doi, H. Honda, Y. Iwamoto, Scintigraphic assessments of the reparative process in osteonecrosis of the femoral head using SPECT/CT with 99mTc hydroxymethylene diphosphonate, Necl. Med. Commun. 35 (2014) 1047–1051.
[22] X. Wang, K. Fukui, A. Kaneuji, K. Hirosaki, H. Miyakawa, N. Kawahara, Inversion of the acetabular labrum causes increased contact pressure on the femoral head: a biomechanical study, Int. Orhop. 43 (2019) 1329–1336.
[23] T.M. Jackman, A.I. Hussein, A.M. Adams, K.K. Makhnejia, E.F. Morgan, Endplate deflection is a defining feature of vertebral fracture and is associated with properties of the underlying trabecular bone, J. Orthop. Res. 32 (2014) 880–886.
[24] Y. Kubo, G. Motomura, S. Ikemura, H. Hatanaka, J.I. Fukushi, S. Hamai, T. Yamamoto, Y. Nakashima, Osteoclast-related markers in the hip join fluid with

subchondral insufficiency fracture of the femoral head, J. Orthop. Res. 36 (2018) 1987–1995.
[25] J.H. Byun, S. Jang, S. Lee, S. Park, H.K. Yoon, B.H. Yoon, Y.C. Ha, The efficacy of bisphosphonates for prevention of osteoporotic fracture: an update meta-analysis, J. Bone Metab. 24 (2017) 37–49.
[26] W. Li, T. Sakai, T. Nishii, N. Nakamura, M. Takao, H. Yoshikawa, N. Sugano, Distribution of TRAP-positive cells and expression of HIF-1alpha, VEGF, and FGF-2 in the reparative reaction in patients with osteonecrosis of the femoral head, J. Orthop. Res. 27 (2009) 694–700.
[27] K. Karasuyama, T. Yamamoto, G. Motomura, K. Sonoda, Y. Kubo, Y. Iwamoto, The role of sclerotic changes in the starting mechanisms of collapse: a histomorphometric and FEM study on the femora head of osteonecrosis, Bone. 81 (2015) 644–648.
[28] J.J. Schreiber, P.A. Anderson, H.G. Rosas, A.L. Buchholz, A.G. Au, Hounsfield units for assessing bone mineral density and strength: a tool for osteoporosis management, J. Bone Joint Surg. Am. 93 (2011) 1057–1063.
[29] S.Y. Lee, S.S. Kwon, H.S. Kim, J.H. Yoo, J. Kim, J.Y. Kim, B.C. Min, S.J. Moon, K.H. Sung, Reliability and validity of lower extremity computed tomography as a screening tool for osteoporosis, Osteoporos. Int. 26 (2015) 1387–1394.
[30] S.J. Lee, P.M. Graffy, R.D. Zea, T.J. Ziemlewicz, P.J. Pickhardt, Future osteoporotic fracture risk related to lumber vertebral trabecular attenuation measured at routine body CT, J. Bone Miner. Res. 33 (2018) 860–867.